Manuscript Details

Manuscript number	MECHMT_2017_107
Title	Principle of operation of RotWWC-VSA, a multi-turn rotational variable stiffness actuator
Article type	Research Paper

Abstract

This work presents the principle of operation of RotWWC-VSA, a Variable Stiffness Actuator (VSA) characterized by no rotational stroke limits, conversely to the vast majority of rotational VSAs, typically characterized by restrictions in the angular range of motion. The possibility to perform an unlimited number of turns is a characteristic taken for granted for standard motors, but it is not for VSA rotational motors. It features two antagonist nonlinear equivalent springs, each of them made up of a tension spring, a cam and a wire which, properly configured, realize a torsion spring characterized by a customizable non-linear stiffness characteristic. Theoretical aspects of the actuator are accompanied by numerical simulations. Design guidelines are drawn and a concept design is presented.

Keywords	Agonist-antagonist variable stiffness actuator; Non-linear torsion spring; Multi-turn rotation; Wrapped spiral cam; Wire-based mechanical transmission

Corresponding Author	Matteo Malosio
Order of Authors	Matteo Malosio, Giulio Spagnuolo, Alessio Prini, Lorenzo Molinari Tosatti, Giovanni Legnani

Submission Files Included in this PDF

File Name [File Type]

Response to the Review Comments MECHMT_2017_107.pdf [Response to Reviewers]

rotwwc_vsa_mmt.pdf [Manuscript File]

Highlights.pdf [Highlights]

To view all the submission files, including those not included in the PDF, click on the manuscript title on your EVISE Homepage, then click 'Download zip file'.

Authors' Response to the Review Comments

Journal: Mechanism and Machine Theory

Manuscript #: MECHMT_2017_107

Title of Paper: Principle of operation of RotWWC-VSA, a multi-turn rotational variable stiffness actuator

Authors: Matteo Malosio, Giulio Spagnuolo, Alessio Prini, Lorenzo Molinari Tosatti, Giovanni Legnani

Date Sent: April 28th, 2017

We greatly appreciate the time and efforts by the editor and referees in reviewing this manuscript. We have addressed the issues indicated in the review report, in the hope that the revised version can meet the journal publication requirements. New contributions are highlighted in red. Language corrections and minor modifications are not highlighted.

Response to Comments from Reviewer 1

Overall Comment

The paper deals with the description of the principle of operation of a rotational variable stiffness actuator based on the use of two antagonist cam-wire springs.

The device under investigation is very similar to the linear variant proposed by the authors in a previous paper (the referenced paper [15]). The main difference is in the final embodiment which allows for the rotational degree of freedom instead for the linear one. Both the architecture are based on the Rotational Wire-Wrapped Cam which is already explained and detailed in the referenced paper [15]. Moreover, also the same methodology of the previous study is extended to the rotational version.

For all these reasons, the paper is more focused to an extension of a known device and methodology rather than to a ground-breaking novelty.

Besides of that, it is well written and the discussed application is of interest in the engineering field. It is almost complete, clear and convincing. For this reason, I am in favour for the publication of the manuscript after a minor revision process.

Response

The authors would like to thank Reviewer 1.

Specific comment 1

Pag. 2 – two lines from the bottom: authors knowledge -> authors' knowledge;

Response

Fixed.

Specific comment 2

The parameters v_1 and v_2 seem not to be defined in the text of in Table 1.

Response

Their meaning has been added within the text in Section 2, with the expression

"with angular coordinate υ_i"

Specific comment 3

The curves in the plots of Figures 10, 11 and 12 are too thin. Please make them thicker.

Response

The curves have been made thicker as suggested.

Specific comment 4

The concept design in Figure 14 deserves a better explanation about the role of each component. Consider promoting the description to a dedicated section of the paper.

Response

A dedicated section ("Concept design of a rotwwcsea-based actuator") has been added as suggested by the reviewer. The description has been extended in order to better explain the role of each component and the related figures have been updated with used nomenclature.

Specific comment 5

In the acknowledgement section it is not clear the source of the founding: who is Telethon? A private or public agency?

Response

The acknowledgment has been fixed. There was an error. The Bridge project is financed by the Italian private non-profit Cariplo Foundation.

Specific comment 6

In the appendix, the hat-script of VE in Eq. 30 differ from the vector style in the other Equations.

Response

In Eq. 30 the double-sided arrow over VE denotes the infinite line passing containing V and E, as reported in Table 1.

The expression

$$d(O_c, \overleftrightarrow{VE})$$

denotes the distance from *O_c* to the line containing V and E. In fact, as reported in Table 1, *d(P,l)* denotes the minimum distance between point P (O_c in (30)) and line *l* (*VE* with the double-sided arrow). By taking this into consideration, the authors do not think it is required to change the notation. If the reviewer is available to suggest any possible alternative, it will be certainly taken into account.

Response to Comments from Reviewer 2

Overall Comment

This manuscript deals with an interesting investigation on the modeling of two antagonist cam-wire systems in a good series of papers by the authors.

Response

The authors would like to thank Reviewer 2.

Specific comment 1

The authors should clearly highly the novelty and main contribution of the work reported here.

Response

One paragraph has been added in Section 1.3, from "Within the present work…" and "…referenced to" to specify the aim and peculiarity of the work, in particular referring to the dual configuration denoted LinWWC-VSA [16].

Specific comment 2

The authors should also comment on the validation and experimental application of the concepts described.

Response

A paragraph explaining the successive steps, the validation and experimental application of the described

concept has been added in the Conclusions section.

Specific comment 3

The English language used in the manuscript must be polished.

Response

The authors revised the paper and hope that the quality of the language has been improved satisfactorily.

Specific comment 4

The literature review in the field must be revised and updated.

Response

The articles entitled:

- "Variable Stiffness Actuators: Review on Design and Components"
- "Coupling between the Output Force and Stiffness in Different Variable Stiffness Actuators"
- "Compliant actuation of parallel-type variable stiffness actuator based on antagonistic actuation"
- "Conceptual Design and Analysis of Four Types of Variable Stiffness Actuators Based on Spring Pretension"

have been updated. We realized that they were not complete. Thank you.

Moreover, the article entitled

- "Mechanical Design and Analysis of the Novel 6-DOF Variable Stiffness Robot Arm Based on Antagonistic Driven Joints"
- "Synthesis of a torsional spring mechanism with mechanically adjustable stiffness using wrapping cams"

have been added among the references.

Specific comment 5

It would be great of the authors provide a complete list of nomenclature.

Response

A List of Nomenclature (Table 2) has been added. It includes the names mostly used within the paper. It neglects, for clearness, symbols and names strictly related to specific figures or equations.

Specific comment 6

The graphical quality of same figures must be improved to facilitate their reading.

Response

Figure from 10 to 12 have been modified with thicker lines.

The concept design of the actuator exploiting the described mechanism (Fig. 14) has been modified adding bullets for a better explanation of its components within the text.

Figure 15 has been updated clarifying points and fixing an error.

Symbols and lines of Figure 6 and Figure 5 have been slightly repositioned and clarified for a better reading.

With the hope of having addressed the issue raised by the reviewer, we'll insert any other required modification.

Specific comment 7

The authors should also discuss the main consequences and implications in terms of design guidelines.

Response

The section entitled "Design guidelines" has been added.

Principle of operation of RotWWC-VSA, a multi-turn rotational variable stiffness actuator

M. Malosio[a,*], G. Spagnuolo[a,b], A. Prini[a], L. Molinari Tosatti[a], G. Legnani[a,b]

[a] *Institute of Industrial Technologies and Automation - CNR, via Alfonso Corti 12, 20133 Milan, Italy*
[b] *University of Brescia, Piazza del Mercato 15, 25121 Brescia, Italy*

Abstract

This work presents the principle of operation of RotWWC-VSA, a Variable Stiffness Actuator (VSA) characterized by no rotational stroke limits, conversely to the vast majority of rotational VSAs, typically characterized by restrictions in the angular range of motion. The possibility to perform an unlimited number of turns is a characteristic taken for granted for standard motors, but it is not for VSA rotational motors. It features two antagonist nonlinear equivalent springs, each of them made up of a tension spring, a cam and a wire which, properly configured, realize a torsion spring characterized by a customizable non-linear stiffness characteristic. Theoretical aspects of the actuator are accompanied by numerical simulations. Design guidelines are drawn and a concept design is presented.

Keywords:
Agonist-antagonist variable stiffness actuator, Non-linear torsion spring, Multi-turn rotation, Wrapped spiral cam, Wire-based mechanical transmission

1. Introduction

1.1. Variable Stiffness Actuators

A Variable Impedance Actuator (VIA) is an actuator which deviates from its set equilibrium position, depending on the external forces and the mechanical properties of the actuator (i.e. inertia, stiffness and damping factors), oppositely to non-VIA (traditional stiff actuator) characterized by excellent trajectory tracking with a high bandwidth and high accuracy [1]. Inherent compliance actuators constitute a subgroup of VIAs, containing passive or intrinsic compliant element in series to the (stiff) actuator. They can be subdivided into Series Elastic Actuators (SEA - Fig. 1a) [2], in which the compliant element does not change its stiffness (fixed compliance), and Variable Stiffness Actuators (VSA - Fig. 1b) [3], in which the stiffness is controlled by mechanical reconfiguration.

VSAs [1] allow the adjustment, in a controlled manner and at the same time, of both the mechanical stiffness and the equilibrium configuration of the load. Peculiar features are

*Corresponding author
Email address: matteo.malosio@itia.cnr.it (M. Malosio)

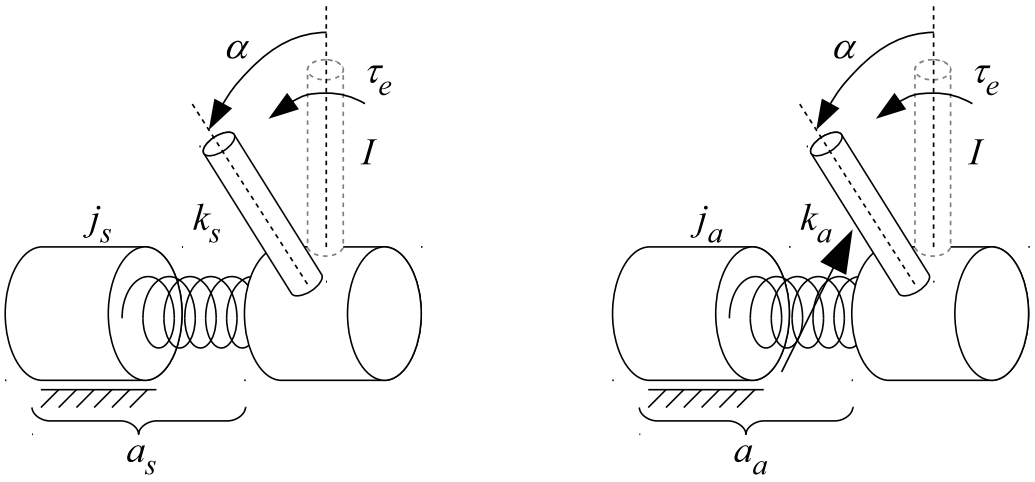

(a) Series Elastic Actuator (SEA). (b) Variable Stiffness Actuator (VSA).

Figure 1: A Series Elastic Actuator a_s is made up of an actuator j_s and a compliant element k_s configured in series. A Variable Stiffness Actuator a_a is characterized by an adjustable compliant element k_a. An external torque τ_e applied to I causes a rotation α.

mechanical stiffness adjustment, adaptability and force accuracy in the interaction with the operator facilitating a direct interaction with humans limiting forces in case of collision, and robustness to external perturbations or model errors [4]. All of them are obtained without necessarily requiring force-based control techniques, favoring mechanical backdrivability, transparency and bandwidth.

For all these aspects, potentially positive in a number of applications, a number of different VSAs have been recently conceived and realized [1, 5, 6]. Moreover, the more and more growing interest in VSAs led Grioli et al. to present a VSA datasheet as an interface language between designers and users and to discuss design procedures and how VSA data may be organized to minimize the engineers effort in choosing the actuator type and size [7]. In order to further support designers in developing new VSA solutions, design guidelines for R&D engineers facing the challenge of designing new VSA systems and implementing them in use-cases as shock absorbing, stiffness variation, cyclic motions and explosive motions are proposed [6].

1.2. Use of rotational VSAs to realize an unlimited number of turns

It is a matter of fact that the vast majority of the so-far developed VSAs perform rotational motions. Nevertheless, if compared to traditional rotational actuators which typically can perform bidirectionally an infinite number of turns, the majority of rotational VSAs are characterized by restrictions in the actually exploitable range of motion. In fact, to the authors' knowledge, only few rotational VSAs have so far being developed featuring an infinite number of turns. Among them it is worth to mention the PVSA [8], the actuator developed by Tonietti et al. [9] and the ComPact-VSA [10]. However, all of them requires a great number of manufactured parts. Moreover, the first two of them are characterized

by the presence of a pin-slot joint which requires precise manufacturing and assembling operations. The vsaUT-II [11] guarantees a large variation of stiffness but requires many manufactured components and mechanical joints as gears and pin-slot joints. Moreover, it is affected by a limited rotational range of motion. The use of profiled surfaces is considered promising to customize the stiffness-displacement curve. Both the VS-Joint mechanism [12] and the third architecture presented by Guo et al. in [13] require a pin-slot joint and good mechanical tolerances. Similar and alternative solutions are presented in [14]. Interesting is AMASC [15] which adopts coupled cams to obtain springs non-linearity.

In order to realize linear motions using rotational actuators, it is common the use of mechanical transmissions based on rack and pinion, pulley and belt, or drum and wire. However, with the purpose of realizing linear actuators with (theoretically) no stroke restrictions, the employed actuators require not to be affected by any rotational limit or end stroke (i.e. they should be able to perform an unlimited number of turns). Summarizing, few rotational VSAs can be effectively exploited for this aim. Moreover, the existing ones are typically characterized by a great number of components and require strict-tolerance machining and assembling operations to avoid backlashes or jammings.

1.3. The Rotational Wire-Wrapped Cam VSA

An interesting solution for the aims of this work is the LinWWC-VSA, proposed by Spagnuolo et al. [16], a VSA architecture designed to perform linear motions with a theoretically infinite stroke. It features two antagonistic SEAs, each of them made up of a cam wrapped by a wire and constrained by a torsion spring. Taking inspiration from its principle of operation, the Rotational Wire-Wrapped Cam VSA (RotWWC-VSA) has been conceived. It is an Agonist-Antagonist VSA (AAVSA) [3, 4] suitable to actuate rotational axes with no restrictions in the actually exploitable range of motion, able to perform an unlimited number of turns. It is made up of two antagonistic RotWWC-SEA, each of them featuring a tension spring, a cam and a wire which, properly configured, realize a torsion spring characterized by a customizable non-linear stiffness characteristic.

The use of a cam wrapped by a wire is considered promising in order to minimize the number of mechanical components, as better described in next sections, simplifying the design and assembly operations, and limiting concentrated mechanical stresses. Examples of employment of this approach are the MACCEPA 2.0 [17], the pnrVSA [18], the one proposed by Shin et al. actuated by pneumatic artificial muscles [19], the NLSs proposed by Schepelmann et al. [20], and the mechanism described in [21]. However, all of them are configured to perform rotational movements characterized by a limited rotational range of motion, conversely to the RotWWC-VSA.

Within the present work, the principle of operation and the analysis of the RotWWC-VSA actuator is presented. It is a mechanism dual with respect to the LinWWC-VSA mechanism presented in [16]. Despite some similarities and some common elements, the mechanism described within this new paper faces a completely different actuation setup and application scenario. While LinWWC-VSA has been conceived to realize an intrinsic variable-stiffness linear actuator embedding the non-linear adjustable stiffness within a linear carriage, RotWWC-VSA realizes a multi-turn VSA. With respect to other rotational VSAs

Table 1: Table of symbols

Symbol	Description
$\{k\}$	Frame of reference
O_k	Origin of $\{k\}$
x_k, y_k	Axes of $\{k\}$
$\overleftrightarrow{AB}$	Infinite line containing A and B
$\overline{AB}$	Segment from point A to point B
$\angle(AOB), \angle(l_1 l_2)$	Counterclockwise angle between points A and B at point O (the vertex) or between lines l_1 and l_2
r_P^k, θ_P^k	Polar coordinates of P wrt $\{k\}$
$d(P, Q)$	Distance between point P and Q (i.e. $\|\overrightarrow{PQ}\|$)
$d(P, l)$	Minimum distance between point P and line l
$a \propto b$	a proportional to b

it is multi-turn, characteristic which is not widespread among rotational VSAs, and realized with relatively simple components without requiring precise manufacturing and assembling operations, as some others previously described. Within this paper, aspects already faced in [16], as numerical and analytical methods to design the cam embedded within the actuator, will not be described in details and will be referenced to.

The work is organized as follows. The list of used symbols is reported in Table 1. A list of nomenclature is reported in Table 2. General aspects about AAVSA are summarized in Section 2. The RotWWC-SEA is analyzed in Section 3. The RotWWC-VSA is illustrated in Section 4. Simulations and related discussions are reported in Section 5. Design guidelines are presented in Section 6. The concept design of a RotWWC-VSA-based actuator is shown in Section 7. Conclusions and future works are drawn in Section 8.

2. General aspects of Agonist-Antagonist VSAs

An Agonist-Antagonist VSA (AAVSA) mimics the principle at the basis of antagonist muscles [22], for which the stronger the antagonistic forces are, the stiffer the articulation becomes [5]. It is made up of two antagonist SEAs, kinematically in parallel with respect to a mobile mass (Fig. 2). The non-linearity of the elastic element is required to allow the adjustment of the VSA stiffness [4].

Referring to Fig. 1 let us denote by a a generic compliant rotational actuator made up of a rigid joint j and a spring s with stiffness k, connected to an inertia I. Let us conveniently denote by the subscripts s and a a SEA (Fig. 1a) and a VSA (Fig. 1b), respectively. Let us denote by α the angular coordinate of I, by α_e its coordinate if no external torque is applied (equilibrium position) and by $\Delta\alpha = \alpha - \alpha_e$ the angular displacement of I from its equilibrium position. The stiffness k of the actuator and the exerted torque τ are expressed by

$$k(\alpha) = \frac{\mathrm{d}\tau}{\mathrm{d}\alpha} \qquad \tau = \int_{\Delta\alpha} k(\alpha)\,\mathrm{d}\alpha. \tag{1}$$

Table 2: List of nomenclature

Symbol	**Description**
H	Minimum-distance point from O_c to a line t tangent to c
I	Rotational inertia
O_c	Center of the cam c
a_a	Agonist-antagonist variable stiffness actuator
b	Distance from O_c to H
$c(r, \theta)$	Cam defined by polar coordinates r and θ
f_l	Force exerted by the tension spring
j_i	i-th joint
k_a	Stiffness of I due to a_a
k_i	Stiffness of j_i
k_l	Stiffness of s_l
k_t	Torsional stiffness
l_l	Length of s_l
p	Pulley
s_l	Tension spring
w	Wire
Γ_{kl}	Ratio between the maximum and the minimum torsional stiffness
β	Pitch angle of the cam profile
δ	Distance between j_i and the equilibrium coordinate υ_e
ξ	Displacement of I from its equilibrium configuration
ρ	Radius of p
τ_a	Torque applied by a_a to I
τ_e	External torque
τ_i	Torque exerted by j_i
τ_t	Torque exerted by w on c
υ_e	Equilibrium coordinate of I
υ_i	Angular coordinate of j_i
υ_m	Angular coordinate of I

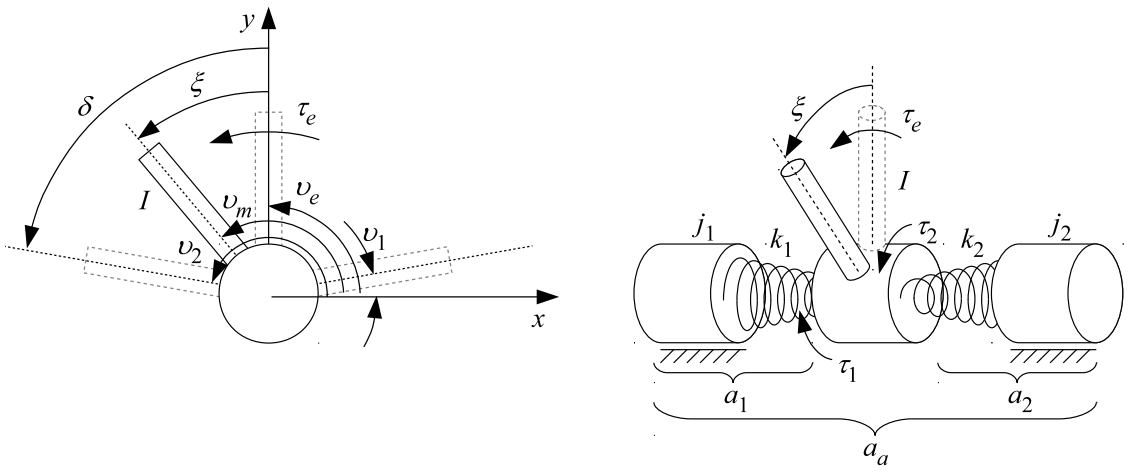

Figure 2: Typical scheme of an antagonistic rotational VSA: two antagonist non-linear SEAs a_i control the orientation and the torsional stiffness of a rotational inertia I.

In static conditions or neglecting inertial effects, it is $\tau_a = -\tau_e$, where τ_a denotes the torque exerted by the actuator and τ_e denotes the external torque. Therefore, by knowing the stiffness-displacement curve of k and the position of I, it is possible to estimate τ_e.

Let us now consider a generic AAVSA a_a made up of two antagonist SEA a_i, with $i = 1, 2$ (Fig. 2). Each a_i is made up of a rigid joint j_i , with angular coordinate υ_i, and a compliant element with stiffness k_i. The antagonistic actuators are connected to an inertia I with position υ_m.

Referring to Fig. 3, the torque applied to I by a_a is

$$\tau_a = \tau_2 + \tau_1 = -\tau_e. \tag{2}$$

Similarly, since the two actuators are in parallel, the stiffness of a_a is

$$k_a = k_2 + k_1. \tag{3}$$

The torque/displacement characteristic of a generic AAVSA, given $k_1 = k_2$, is represented in Fig. 3. The equilibrium position of I is determined by the value $-\tau_e$ along the curve τ_a (neglecting inertial effects). If no external torque is applied (i.e. $\tau_e = 0$), the position of I is

$$\upsilon_e = (\upsilon_1 + \upsilon_2)/2. \tag{4}$$

Let us conveniently denote

$$\delta = (\upsilon_2 - \upsilon_1)/2 \qquad \xi = \upsilon_m - \upsilon_e \tag{5}$$

used in the next sections as the two independent coordinates of a AAVSA. It is worth to underline that, if δ and ξ are known, together with the spring stiffness $k(\alpha)$, it is straightforward to deduce τ_e.

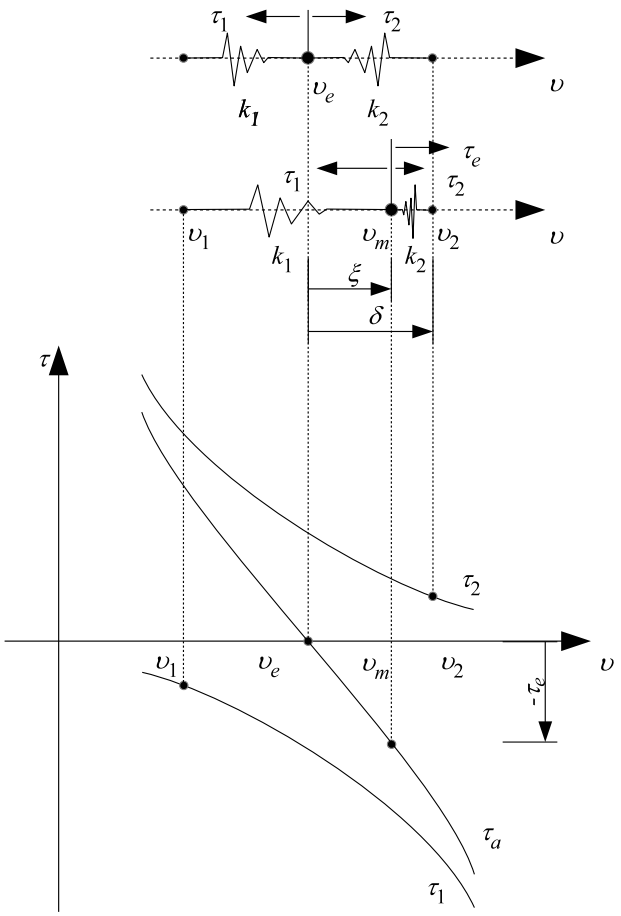

Figure 3: Torque characteristic of a VSA as function of coordinates υ_1, υ_2 of springs k_1, k_2 and of the external torque τ_e.

3. RotWWC-SEA

Referring to Fig. 4, let us consider a cam defined by the curve $c(r, \theta)$ wrt the reference frame $\{c\}$. Let us conveniently consider a cam shaped as a spiral, with r monotonically increasing wrt θ. Let us denote by $A(r_A, \theta_A)$ and $B(r_B, \theta_B)$ the points of the cam with the minimum and maximum values of r, respectively. It is $r_A \leq r \leq r_B$ and $\theta_A \leq \theta \leq \theta_B$. Considering a point $T \in c$, let us denote by t the line passing through T and tangent to c, and by H the point on t at minimum distance b from O_c.

As it is known in geometry, the curvilinear coordinate of $T(r_T, \theta_T)$ along the cam profile is

$$s_T^A = \int_{\theta_A}^{\theta_T} \mathrm{d}s = \int_{\theta_A}^{\theta_T} \sqrt{r^2 + \left(\frac{\mathrm{d}r}{\mathrm{d}\theta}\right)^2}\, \mathrm{d}\theta, \tag{6}$$

the pitch angle β, complement of the angle between t and r, is equal to

$$\beta = \angle(HO_cT) = \arctan\left(\frac{1}{r}\frac{\mathrm{d}r}{\mathrm{d}\theta}\right), \tag{7}$$

and the minimum distance between t and O_c is

$$b = \overline{O_c H} = r \cos \beta. \tag{8}$$

Let us consider a cam c as the one depicted in Fig. 5. The cam is wrapped by a wire w having an endpoint constrained to A and the other denoted by S. Let us consider w split in two parts by T, i.e. the tangent point on the cam, resulting in $w = w_c + w_f$, with w_c wrapped on the cam between A and T, and w_f between T and S, denoting by w both the wire and its length for brevity. A tension spring s_l, with length l_l and stiffness k_l, has one endpoint hinged to S and the other E free to move without friction on a circumference centered in O_c and with radius r_E. Let us conveniently assume as reference configuration the one in which $T \equiv A$ and denote by the superscript ^{0} any parameter referred to it (e.g. P^0 is the position of the generic point P if $T \equiv A$). The reference configuration is represented in Fig. 5 by a dotted line. Considering the cam configured as a spiral with $r_A \leq r \leq r_B$, in this reference configuration s_l assumes its shortest length l_l^0. Let us denote the angular displacement of E from the reference configuration by

$$\Delta\gamma = \gamma - \gamma^0 = \angle(E_0 O_c E) \tag{9}$$

where $\gamma = \angle(A O_c E)$ and $\gamma^0 = \angle(A O_c E^0)$. As $\Delta\gamma$ increases, the wire w_c wrapped on the cam is compensated by the elongation of s_l

$$\Delta l_l = l_l - l_l^0. \tag{10}$$

The total length of the wire and of the spring from A to E is

$$\begin{aligned} l &= w + l_l \\ &= w_c + w_f + l_l \\ &= w_c + \overline{TE}, \end{aligned} \tag{11}$$

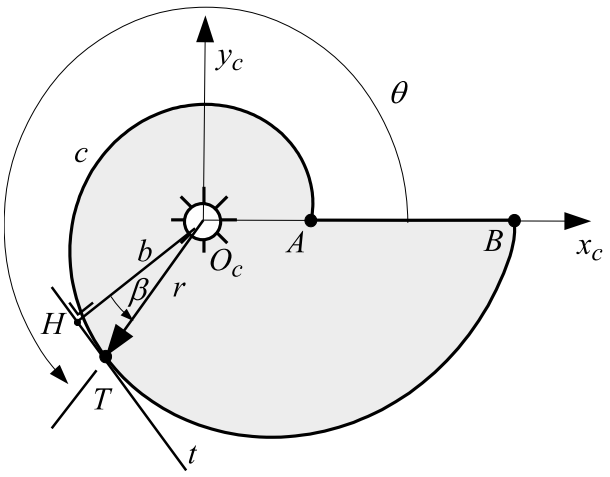

Figure 4: Spiral cam profile.

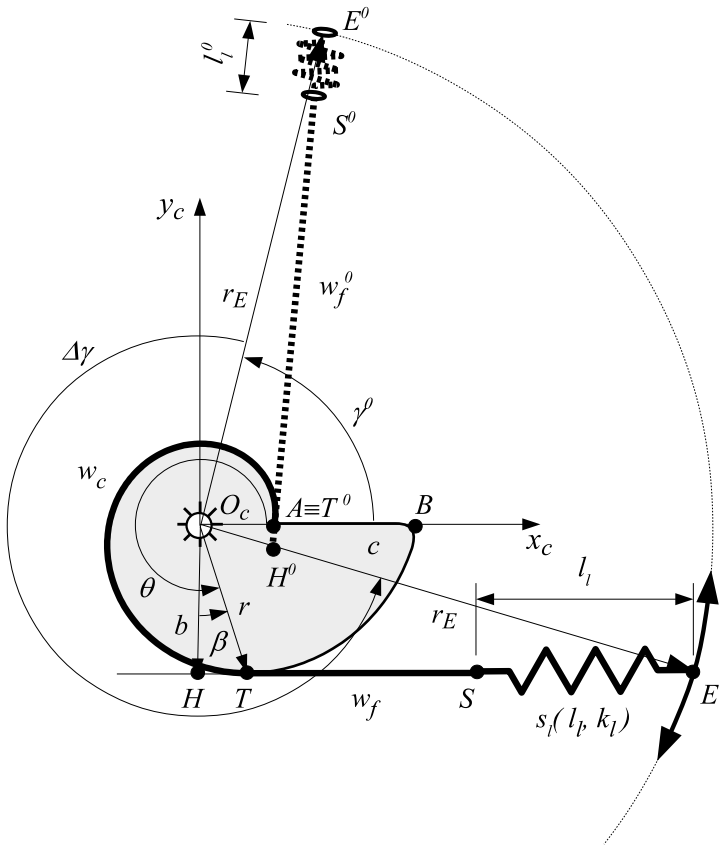

Figure 5: The Rotational cam-based VSA. The thicker line represents the wire w and the spring s_l.

where

$$\begin{aligned}\overline{TE} &= \overline{HE} - \overline{HT} \\ &= \sqrt{r_E^2 - b^2} - r\sin\beta. \end{aligned} \tag{12}$$

Therefore

$$\begin{aligned}\Delta l_l &= (w_c + w_f + l_l) - (w_f^0 + l_l^0) \\ &= w_c + (\overline{HE} - \overline{HT}) - (\overline{H^0E^0} - \overline{H^0A}). \end{aligned} \tag{13}$$

The spring s_l generates a tension force f_l function of l_l and of its force-displacement characteristic. Let us assume, for simplicity, it to be a common tension coil spring with a constant stiffness k_l and exerting no force if $l_l = l_l^0$, i.e. its equilibrium configuration. The exerted force is therefore

$$f_l = \int_{\Delta l_l} k_l \,\mathrm{d}l_l = k_l \Delta l_l. \tag{14}$$

The resultant torque τ_t applied to c by w is

$$\tau_t = \int_{\Delta\gamma} k_l b^2 \,\mathrm{d}\gamma. \tag{15}$$

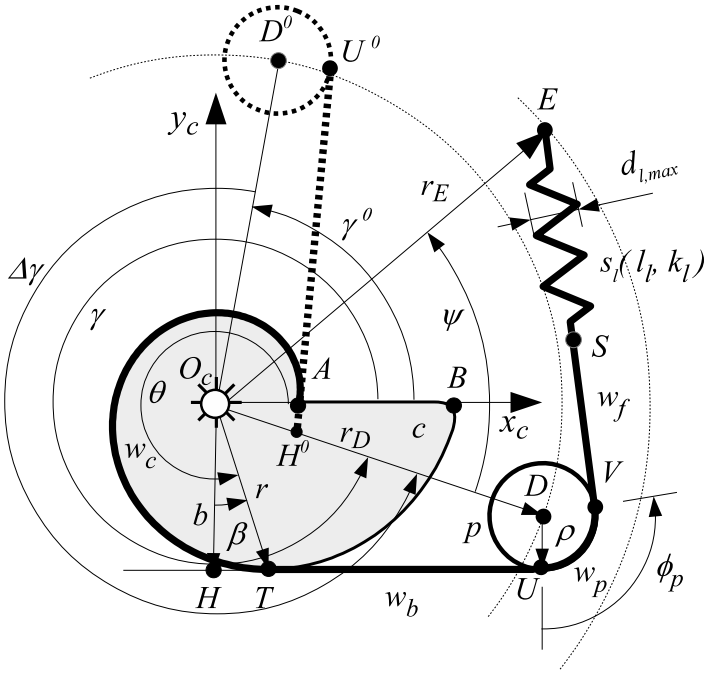

Figure 6: The RotWWC-SEA configured with a pulley to reduce its dimensions.

Therefore, the mechanism realizes a customizable non-linear torsion spring properly dimensioning parameters of the cam and of the spring.

In order to avoid s_l to get in contact with the cam, the condition $w \geq s_B^A = w_{min}$ must be respected, where s_B^A is the curvilinear length of the cam profile from A to B. This condition guarantees that only w is wrapped on the cam and that s_l does not get in contact with c.

A drawback of the architecture so far presented is its overall dimensions. In fact, given c and therefore w_{min}, r_E must be such as to ensure that $\overline{AE^0} \geq w_{min} + l_l^0$.

In order to obtain a more compact design without modifying the principle of operation of the mechanism, the system can be arranged as in Fig. 6. The wire w is deflected by a pulley p, centered in D and with radius ρ, leading to reduce $\overline{O_cE}$. Analytic details are reported in the Appendix.

It must be noted that a couple of geometric constraints must be satisfied to obtain a physically realizable and functioning mechanism. In order not to have s_l wrapped on p, it is necessary to guarantee that $\overline{VE} \geq l_{l,max}$, where $l_{l,max}$ denotes the maximum required length of s_l. Moreover, not to have p colliding against c, it must be $r_D \geq r_B + \rho$. Another condition to be respected is that

$$d(O_c, \overleftrightarrow{VE}) > r_B + d_{l,max}/2, \tag{16}$$

where $d_{l,max}$ is the maximum diameter of s_l.

4. RotWWC-VSA

Applying the principle of operation depicted in Fig. 2, it is possible to configure two antagonistic RotWWC-SEAs to realize a RotWWC-VSA. The RotWWC-SEA has been represented in Section 3, assuming the cam as fixed with respect to the absolute frame of reference and the free endpoint of the wire E rotating about the center of the cam. Oppositely, let us hereafter consider two cams c_1 and c_2 rigidly constrained to an inertia I which can rotate around the axis z, as depicted in Fig. 7. For clearness of representation, the configuration without the pulley (Fig. 5) is reported. The following reasoning is, however, valid also for the configuration depicted in Fig. 6.

Referring to Fig. 7, the points E_1 and E_2 can rotate around z at constant distances $r_{E,1}$ and $r_{E,2}$, respectively. Similarly to Fig. 5, let us denote by E_1^0 and E_2^0 the position of E for which no force is exerted by the springs. Consequently, modifying the angles $\Delta\gamma_1$ and $\Delta\gamma_2$ two opposite torques τ_1 and τ_2 are applied to I. These two opposite torques allow to actuate I around z, similarly to the scheme depicted in Fig. 2.

Referring to (5), the quantities defining the pretension of the system and the displacement with respect to its equilibrium configuration are, respectively,

$$\delta = (\Delta\gamma_1 + \Delta\gamma_2)/2 \qquad \xi = (\theta_1 - \theta_2)/2, \tag{17}$$

with the subscript i denoting the i-th RotWWC-SEA. In Fig. 8, the RotWWC-VSA is represented in four different configurations, with different values of δ and ξ. The depicted configurations show the principle of operation of RotWWC-VSA, which enables to control

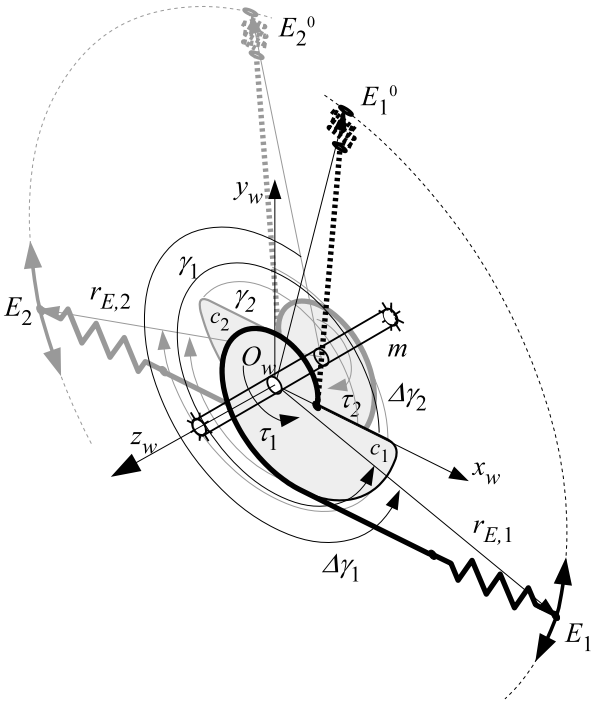

Figure 7: Two antagonist RotWWC-SEA feature the RotWWC-VSA.

Table 3: Parameters of a RotWWC-SEA with a logarithmic spiral.

Parameter	Description	Value	Unit
Γ_{kl}	Ratio between maximum and minimum stiffness	10	–
r_B	Maximum radius of the cam	1	m
$\Delta\theta$	Angular extension of the cam	2π	rad
c_1	Constant of the logarithmic spiral	0.316227	m
c_2	Constant of the logarithmic spiral	0.183236	rad^{-1}
r_D	Distance $\overline{O_cD}$	2	m
r_E	Distance $\overline{O_cE}$	2.5	m
ψ	Angle $\angle(DO_cE)$	2	rad
ρ	Radius of pulley p	0.2	m
k_l	Stiffness of the linear spring	1	$\mathrm{N\,m}^{-1}$

the equilibrium orientation of the rotating inertia I and its torsional stiffness, controlling the positions of E_1 and E_2 with respect to the absolute reference frame.

5. Analysis of the RotWWC-VSA and discussion

Let us now consider a numerical example to better analyze the principle of operation of the actuator, considering a RotWWC-VSA made up of two antagonist RotWWC-SEA featuring logarithmic spirals. As explained in [16], the logarithmic spiral is beneficial from the design point of view, since it allows an analytic definition of the cam profile on the basis of convenient parameters from an engineering point of view. In particular, as detailed in [16], in order to realize a non-linear spring realized by a cam wrapped by a wire featuring a ratio Γ_{kl} between the maximum and the minimum stiffness, it is possible to design it as the logarithmic spiral

$$r = c_1 e^{c_2 \theta}, \tag{18}$$

with

$$c_2 = \frac{\ln(\Gamma_{kl})}{2\Delta\theta} \qquad c_1 = \frac{r_B}{e^{c_2 \Delta\theta}}, \tag{19}$$

denoting by $\Delta\theta = \theta_B - \theta_A$ the angular span of the cam and by r_B its maximum radius. The considered spiral is configured with the parameters reported in Table 3. The apparently questionable unit values of $r_B = 1\,\mathrm{m}$ and $k_l = 1\,\mathrm{N\,m}^{-1}$, which represent a relatively big cam and compliant tension spring if compared to typical geometric and stiffness data characterizing mechatronic solutions, have been adopted as normalized values. In fact, the numerical results illustrated hereafter can be straightforwardly applied for other values of r_B and k_l taking into account that

$$\Delta l_l \propto r_B; \qquad f_l \propto k_l r_B; \qquad \tau_t, \tau_a, k_t, k_a \propto k_l r_B^2. \tag{20}$$

A simulation of the RotWWC-SEA as function of different values of θ_T is represented in Fig. 9. As T moves from A to B along the cam, the elongation of the spring s_l (represented

by a dotted line) and the rotation $\Delta\gamma$ increase. It is notable that the pulley p reduces the overall dimensions of the mechanism.

The kinematic relationship between $\Delta\gamma$, i.e. the rotation of E and D about O_c, and the elongation of the spring Δl_l is represented in Fig. 10. It can be considered as the transmission ratio of the mechanism.

In Fig. 11 the two stiffnesses of the mechanism are represented. The linear stiffness k_l is the same reported in Table 3 and is independent on $\Delta\gamma$, as expected. The non-linear stiffness k_t of the virtual torsion spring acting on c is determined by the actual shape of the cam. The ratio between the maximum and the minimum stiffness Γ_{kl} is due to the cam profile and is obtained applying the method detailed in (18), (19) and [16].

The torque and force exerted by the tension spring and by the virtual torsion spring are evaluated by (14) and (15), represented in Fig. 12.

Let us now refer to RotWWC-VSA, i.e. the coupled effect of two antagonistic RotWWC-SEA. The surfaces representing the torque applied to and the stiffness of the mobile rotational inertia I, as function of δ and ξ, are depicted in Fig. 13. The stiffness k_a grows with the growth of δ, keeping ξ constant. The maximum value of τ_a is achieved with the highest value of ξ, with $\delta = \xi$. The maximum value of k_a is achieved with the highest value of δ with $\xi = 0$. The maximum theoretical stiffness cannot therefore be exploited rotating I from its equilibrium position. Zero values of τ_a and k_a refer to not allowed configurations. In fact, it is notable the main drawback of this type of actuator: the actually exploitable range of motion depends on δ, similarly to LinWWC-VSA. The limits of ξ are due to the fact that the two RotWWC-SEA reach their endstrokes (i.e. $T \equiv A$ or $T \equiv B$) independently and according to their actual values of $\Delta\gamma$. The maximum and the minimum values of stiffness of RotWWC-VSA are therefore not actually exploitable configurations, since no displacement of I is allowed.

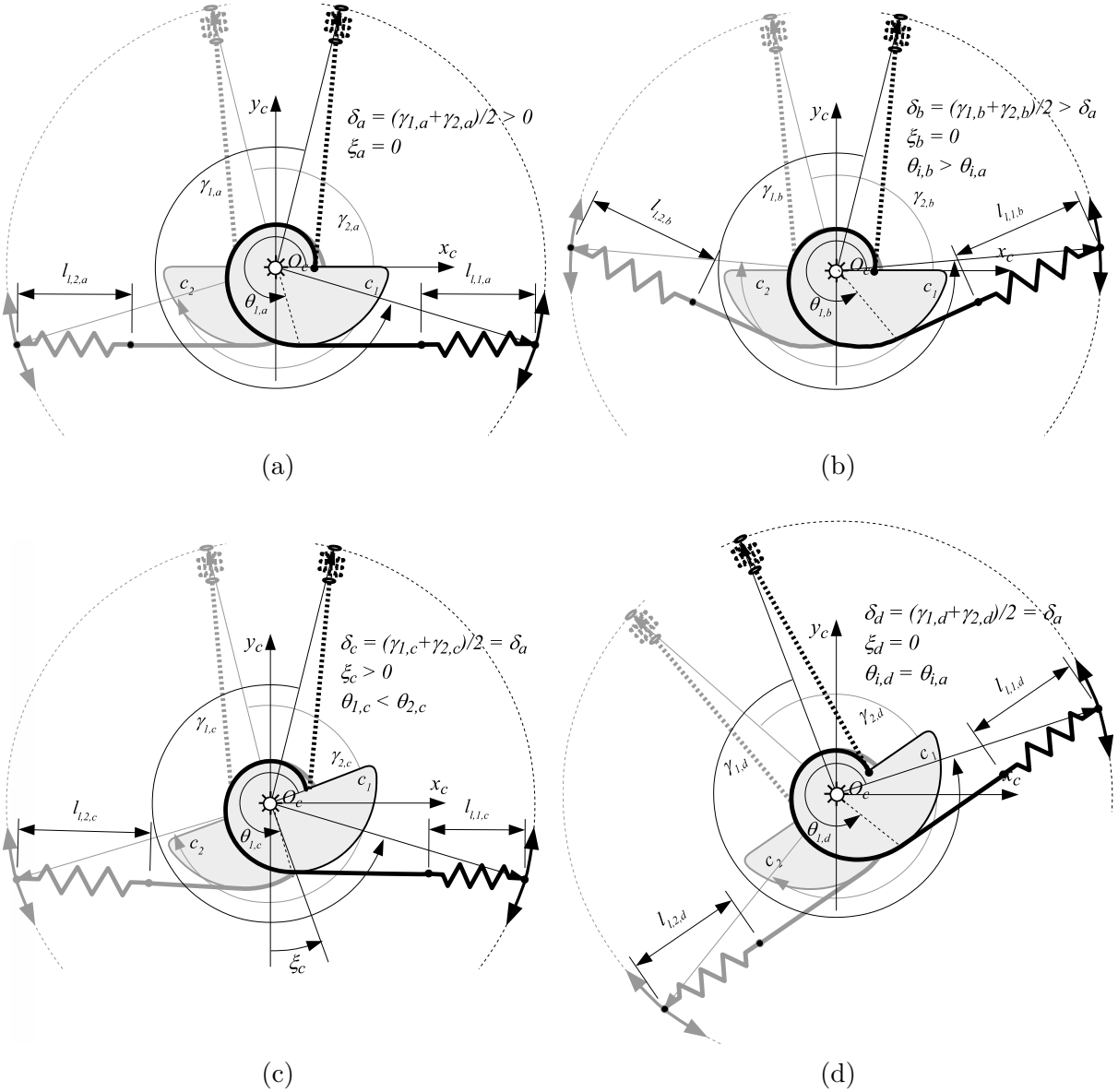

Figure 8: Principle of operation of the RotWWC-VSA depicted in four emblematic configurations. The letter from a to d in subscripts identifies the configuration. Configuration (b) is stiffer than (a); both of them are at the equilibrium configuration with no external torque applied. Configuration (c) has the same stiffness of (a) at the equilibrium and an external torque deflects it from the equilibrium by ξ_c. Configuration (d) has the same stiffness of (a) and the shaft is rotated due to a synchronous movements of the free springs endpoints around O_c.

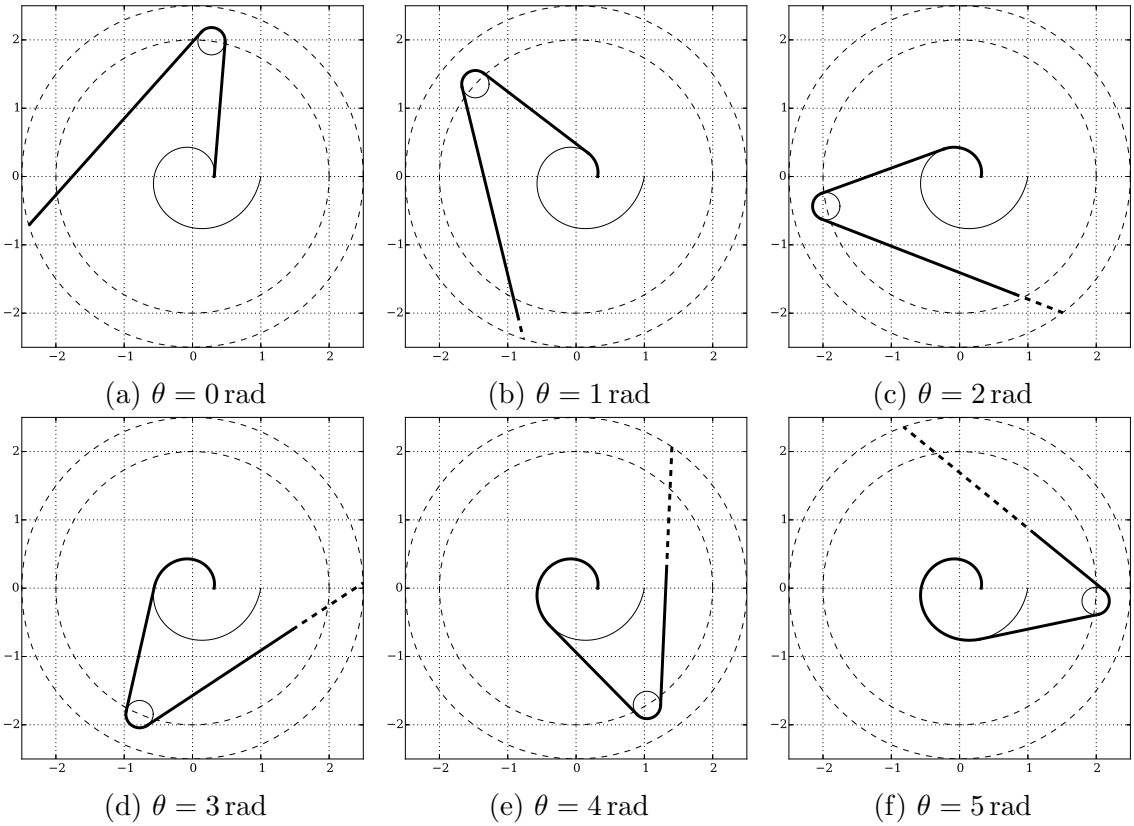

(a) $\theta = 0\,\text{rad}$ (b) $\theta = 1\,\text{rad}$ (c) $\theta = 2\,\text{rad}$

(d) $\theta = 3\,\text{rad}$ (e) $\theta = 4\,\text{rad}$ (f) $\theta = 5\,\text{rad}$

Figure 9: Simulation of RotWWC-SEA cam wrapping with different wrapping angles θ. The tension spring is represented by a dashed line.

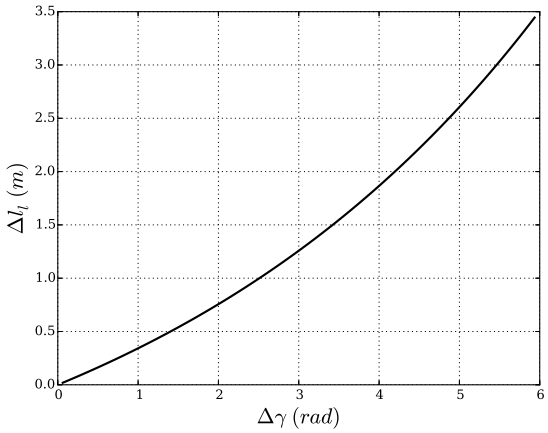

Figure 10: Spring elongation Δl_l as function of the rotation of D wrt O_c.

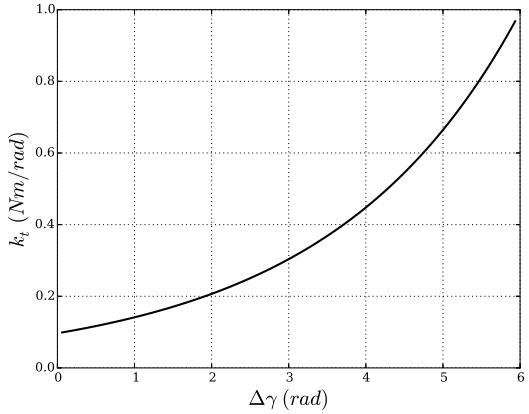

(a) Torsional stiffness of the SEA.

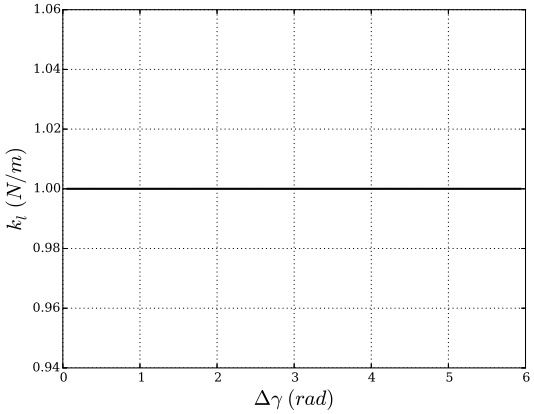

(b) Linear stiffness of the linear spring.

Figure 11: Stiffness as function of the angular displacement of D. The stiffness non-linearity, required to realize a VSA and obtainable by the cam-based transmission mechanism, is notable.

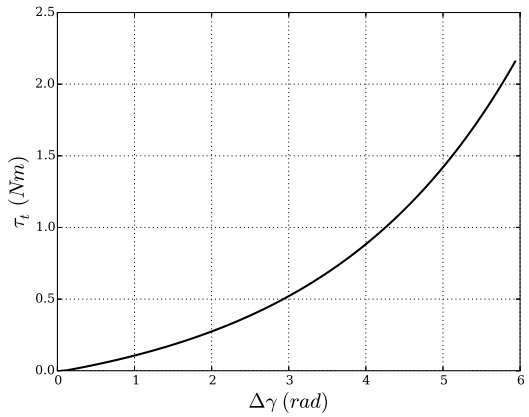

(a) Torque exerted to the cam.

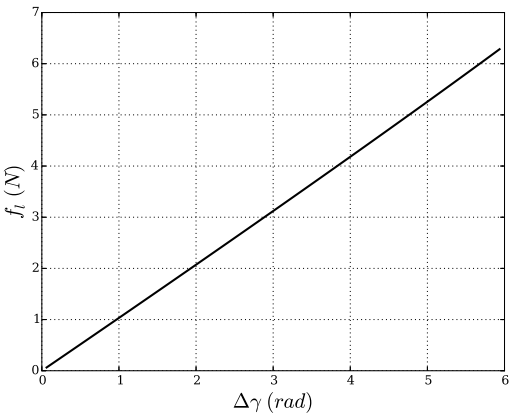

(b) Force exerted by the linear spring.

Figure 12: Force and torque as function of the angular displacement of D.

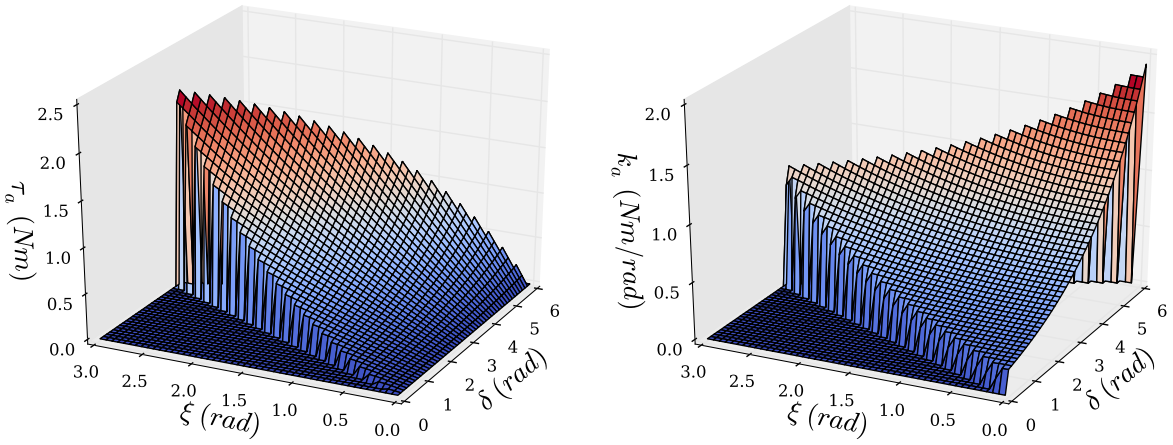

(a) Torque on I.

(b) Torsional stiffness of I.

Figure 13: Torque and torsional stiffness of the rotational inertia I as function of δ and ξ.

6. Design guidelines

The description of the mechanism, the analysis and the discussion carried out in previous sections lead to draw some general guidelines to design actuators based on the architecture described within this paper.

Γ_{kl} is function of the minimum and maximum distances and of the tangent t to the cam profile. Therefore, given Γ_{kl}, in order to reduce the overall dimensions of the cam, it is beneficial to minimize the minimum radius of the cam r_A, given a certain β. This also leads to reduce the maximum dimension of the cam r_B. Nevertheless, it is a matter of fact that, given a desired rotational stiffness k_t and output torque τ_t, the reduction of the dimensions of the cam leads to an increase of the linear spring stiffness k_l and of the force f_l, and consequently of the reaction forces of the pivot center point O_c. At the limit, if $r_A \to 0$, it results that $k_l \to \infty$ and $f_l \to \infty$, which is obviously practically impossible. Therefore, during the design phase, it is required to achieve a compromise between the beneficial aspect of reducing the overall dimensions of the cam (and therefore of the actuator) and of limiting the maximum values of forces and stiffness within feasible limits of physically realizable components.

An additional constraint has to be taken into account. It is a matter of fact that the minimum radius of curvature of the cam and the radius of the pulley p have to be greater than or equal to the minimum radius of curvature allowed by the used wire w, not to damage it. Since a reduction of the dimensions of cam leads to an increase of the wire tension force f_l, this leads to use a thicker wire which, given a defined material, generally means a greater allowable minimum radius of curvature of the wire. This fact, therefore, influences the minimum radius of curvature of the cam and of the pulley, defining another constraint to the minimum allowable dimensions of the actuator.

On the other side, in order to obtain a relatively low rotational stiffness, an increase of the overall dimensions can be beneficial but this solution has to be compatible with installation requirements of the specific target application.

Finally, it must be taken into account that, as highlighted in Fig. 13, if δ tends to zero or to its maximum, the actually exploitable angle of rotation due to an external torque ξ tends to zero. Therefore, the actually exploitable rotation should be taken into account while designing the profile of the cam.

7. Concept design of a RotWWC-SEA-based actuator

The concept design of an actuator embedding the RotWWC-VSA architecture is presented in Fig. 14. It features two input shafts s_i, actuated by two external and generic stiff motors, and one output shaft s_o, connected to the so-far described mechanism and characterized by a variable rotational stiffness.

The concept design of the mechanism which realizes a RotWWC-SEA (Fig. 6) is reported in Fig. 14a. Each input shaft s_i makes E, which is one of the endpoints of each spring k_l, to rotate around O. The mechanical transmission is realized through a synchronous belt t connecting the pulley p_1, rigidly connected to the input shaft, with the pulley p_2, rigidly connected to E through the disc d. The free endpoint of k_l is constrained to the wire w, wrapped on the pulley p and constrained to A, the minimum-radius point of the cam c.

Two RotWWC-SEA mechanisms are assembled within a case in such a way that the two cams are assembled on the output shaft s_o. Each input shaft s_i, supported by bearings b_i, exerts a torque on each cam through the wire w, leading to obtain a couple of antagonist torques on s_o, supported by bearings b_o. The rotation of the discs d, which supports the endpoints E and make them to rotate around the output shaft s_o, is allowed by bearings b_s.

The so-far described concept design allows to put into practice and to realize the principle of operation of the RotWWC-VSA described in the paper and depicted in Fig. 7.

8. Conclusions

The RotWWC-VSA is an agonist-antagonist variable stiffness actuation scheme specifically conceived for realizing rotational actuators performing an infinite number of turns. RotWWC-VSA is a rotational VSA made up, similarly to LinWWC-VSA [16], of two spiral-shaped antagonist cams, each of them wrapped by a wire. As opposed to LinWWC-VSA, the cams are rigidly constrained to the output rotational axis of the actuator, the compliant element (a linear tension spring) has its endpoints constrained to the free endpoint of the wire and on a circumference concentric with the output axis, respectively. If compared to other existing rotational VSAs, RotWWC-VSA is characterized by the peculiarity of having no limitation in the amplitude of rotation, enabling it to freely rotate the load for a whatever number of revolutions, as a traditional rotational actuator. The eventual presence of an optional pulley allows to obtain a more compact solution. It is characterized by a relatively simple set of components and does not require strict manufacturing tolerances. If required by application constraints, in order to either reduce the overall dimensions of the mechanism

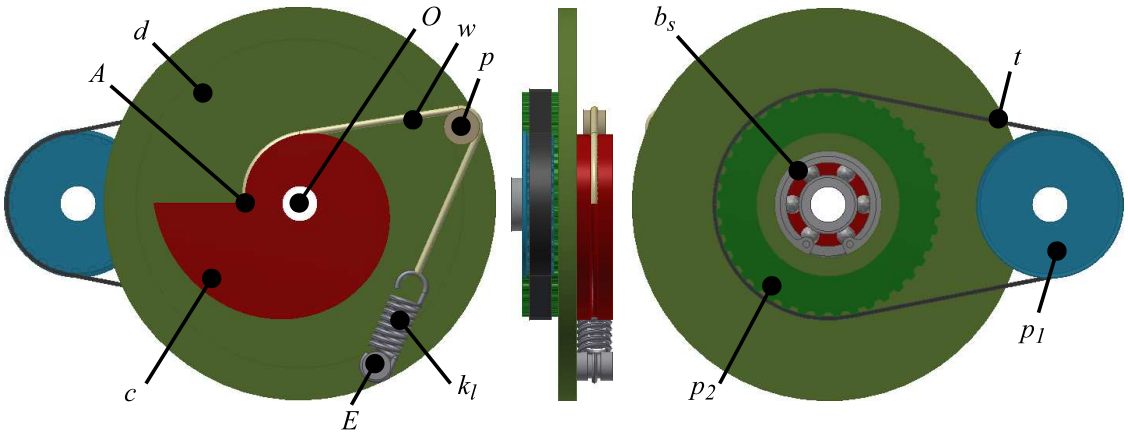

(a) Views of the RotWWC-SEA.

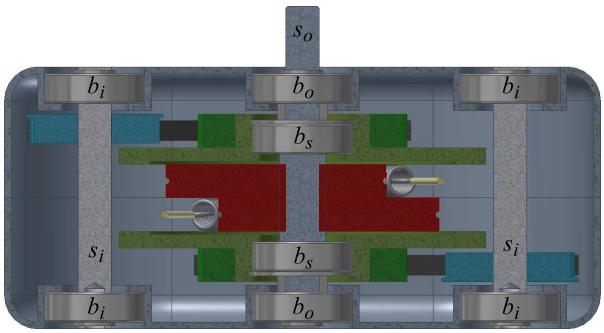

(b) Section top view of the RotWWC-VSA.

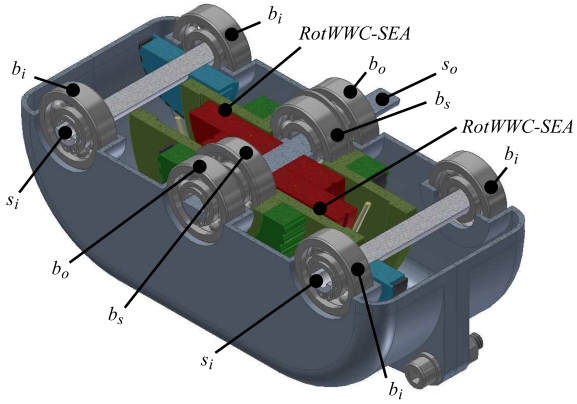

(c) Section 3d view of the RotWWC-VSA.

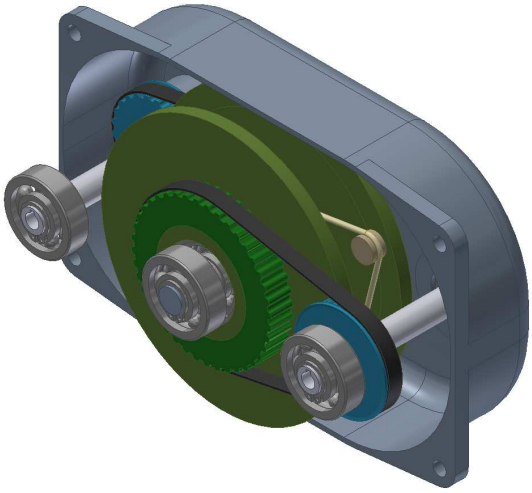

(d) Open view of the RotWWC-VSA.

(e) The RotWWC-VSA completely assembled.

Figure 14: Concept design of an actuator embedding the RotWWC-VSA architecture.

or to modify the rotational range of motion of the actuator, it can be convenient to employ multiple-turns spiral cams, as presented in [16]. Moreover, the presented actuation scheme is suitable to realize compliant linear actuators which, applying proper rotational-to-linear motion transmissions, typically require not to have any endstroke on the employed rotational actuators.

The first prototype of a variable stiffness actuator embedding the mechanism described in this paper is currently in its assembly phase. It will be employed to actuate the shoulder flexion degree of freedom of an assistive exoskeleton. In addition to the analysis of its applicability and efficacy in this specific application and domain, the actuator will be assessed and experimentally characterized per se. The control of the actuator will embed admittance-based control algorithms. The externally applied torque will be inferred by measuring the angular displacement of the output shaft with respect to its equilibrium configuration, as explained at the end of Section 2, after having experimentally obtained the actual torque/displacement characteristic of the actuator. Stiffness, torque, bandwidth, frictions and the characteristics reported in Figures from 10 to 13, calculated by simulation in this paper, will be obtained by experiments and will be embedded within the controller to have a control based on actual mechanical performances and not merely theoretical.

9. Appendix

In this appendix the analytic details of the RotWWC-SEA configured with a pulley, to obtain a more compact solution, are reported.

Referring to Fig. 6 the wire w is constrained to the cam in A and to s_l in S, similarly to Fig. 5. The other endpoint of s_l is E. Let us assume that D and E can rotate about O_c at constant distances r_D and r_E, respectively. Moreover, let us consider that the angle $\psi = \angle(DO_cE)$ is constant. These conditions lead to consider them as rigidly constrained to each other. Similarly to the mechanism depicted in Fig. 5, the elongation of spring s_l is given by (10).

The wire w can be ideally split into four parts, $w = w_c + w_b + w_p + w_f$:

- w_c is wrapped on c, between A and T. It is $w_c = s_T^A$, where s_T^A is the length of the cam wrapped by w_c, from A to T.
- w_b is between T on c and U on p. It is
  $w_b = \overline{HU} - \overline{HT}$, where
  $\overline{HU} = \sqrt{r_D^2 - (b-\rho)^2}$
  $\overline{HT} = r \sin\beta$.
- w_p is wrapped on p, between U and V. It is $w_p = \rho\phi_p$, where $\phi_p = \angle(UDV)$.
- w_f is between V and S. It is
  $w_f + l_l = \overline{VE} = \sqrt{\overline{DE}^2 - \overline{DV}^2}$, where
  $\overline{DE}^2 = r_D^2 + r_E^2 - 2r_D r_E \cos\psi$
  $\overline{DV}^2 = \rho^2$.

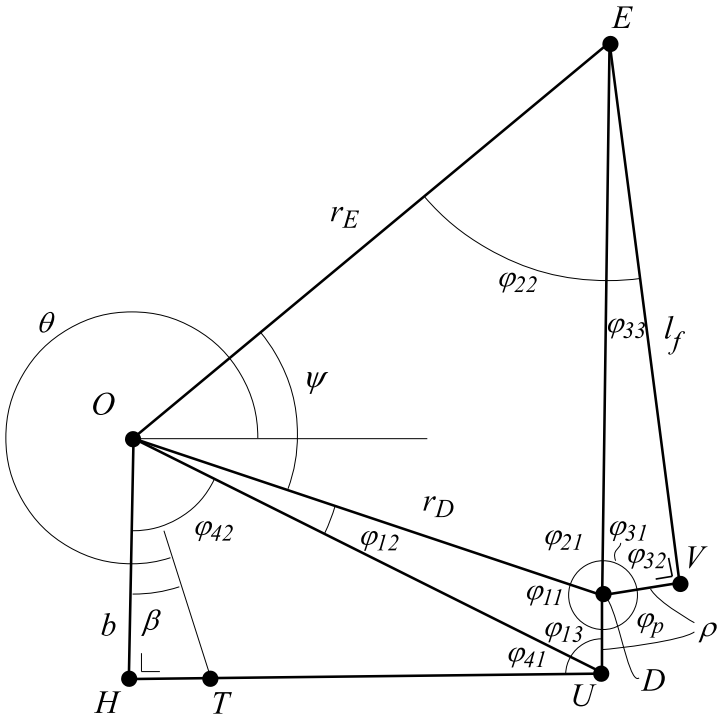

Figure 15: Angles of the RotWWC-SEA featuring an additional pulley.

Let us refer to Fig. 15 to evaluate ϕ_p. It is

$$\phi_p = 2\pi - \phi_{11} - \phi_{21} - \phi_{31} \tag{21}$$

where

$$\phi_{11} = \begin{cases} \phi_{11}^*, & \text{if } \rho > b \\ \pi - \phi_{11}^*, & \text{otherwise} \end{cases} \tag{22}$$

$$\phi_{11}^* = \arcsin\left(\frac{\overline{OU}}{\overline{OD}}\sin\phi_{13}\right) = \arcsin\left(\frac{\overline{OU}}{r_D}\sin\phi_{13}\right) \tag{23}$$

$$\phi_{21} = \arcsin\left(\frac{\overline{OE}}{\overline{DE}}\sin\psi\right) = \arcsin\left(\frac{r_E}{\overline{DE}}\sin\psi\right) \tag{24}$$

$$\phi_{31} = \arccos\left(\frac{\overline{DE}^2 + \overline{DV}^2 - \overline{VE}^2}{2\overline{DE}\,\overline{DV}}\right) = \arccos\left(\frac{\overline{DE}^2 + \rho^2 - \overline{VE}^2}{2\overline{DE}\,\rho}\right) \tag{25}$$

$$\overline{OU} = \sqrt{b^2 + \overline{HU}^2} \tag{26}$$

$$\phi_{13} = \pi/2 - \arctan(b/\overline{HU}) \tag{27}$$

Both w_p and $\overline{EV}$ are constant and defined by construction. Therefore, similarly to (13) starting from the reference position $T \equiv A$, the elongation of the spring s_l is

$$\Delta l_l = w_c + (\overline{HU} - \overline{HT}) - (\overline{H^0U^0} - \overline{H^0A}). \tag{28}$$

Referring to Fig. 6 and Fig. 15 it is possible to evaluate the rotation of D, and therefore E, about the center of the cam. Denoting by γ the rotation of $\overline{O_cD}$ wrt x_c, it is

$$\gamma = \theta - \beta + \phi_{42} + \phi_{12}, \tag{29}$$

where $\phi_{42} = \arctan(\overline{HU}/b)$ and $\phi_{12} = \pi - \phi_{11} - \phi_{13}$. Let us consider

$$\Delta\gamma = \gamma - \gamma^0 \tag{30}$$

as the measure of the angular displacement of the equivalent torsion spring.

Acknowledgments

This work was partially supported by the Italian private non-profit Cariplo Foundation within the BRIDGE project - Behavioural Reaching Interfaces during Daily antiGravity Activities through upper limb Exoskeleton.

The authors would like to thank João Carlos Dalberto and Roberto Bozzi for the support to the mechanical design and the realization of the actuator developed within the BRIDGE project, embedding the principle of operation of RotWWC-VSA.

References

[1] B. Vanderborght, A. Albu-Schaeffer, A. Bicchi, E. Burdet, D. G. Caldwell, R. Carloni, M. Catalano, O. Eiberger, W. Friedl, G. Ganesh, M. Garabini, M. Grebenstein, G. Grioli, S. Haddadin, H. Hoppner, A. Jafari, M. Laffranchi, D. Lefeber, F. Petit, S. Stramigioli, N. Tsagarakis, M. Van Damme, R. Van Ham, L. C. Visser, and S. Wolf, "Variable impedance actuators: A review," *Robot. Auton. Syst.*, vol. 61, no. 12, pp. 1601–1614, Dec. 2013. doi: 10.1016/j.robot.2013.06.009

[2] G. Pratt and M. Williamson, "Series Elastic Actuators," in *Intelligent Robots and Systems 95. 'Human Robot Interaction and Cooperative Robots', Proceedings. 1995 IEEE/RSJ International Conference on*, vol. 1, Aug. 1995. doi: 10.1109/IROS.1995.525827 pp. 399–406.

[3] K. Laurin-Kovitz, J. Colgate, and S. Carnes, "Design of components for programmable passive impedance," in *Robotics and Automation, 1991. Proceedings., 1991 IEEE International Conference on*, Apr 1991. doi: 10.1109/ROBOT.1991.131824 pp. 1476–1481 vol.2.

[4] A. Jafari, "Coupling between the output force and stiffness in different variable stiffness actuators," *Actuators*, vol. 3, no. 3, pp. 270–284, 2014.

[5] R. Ham, T. Sugar, B. Vanderborght, K. Hollander, and D. Lefeber, "Compliant actuator designs," *Robotics Automation Magazine, IEEE*, vol. 16, no. 3, pp. 81–94, Sep 2009. doi: 10.1109/MRA.2009.933629

[6] S. Wolf, G. Grioli, O. Eiberger, W. Friedl, M. Grebenstein, H. Hppner, E. Burdet, D. G. Caldwell, R. Carloni, M. G. Catalano, D. Lefeber, S. Stramigioli, N. Tsagarakis, M. V. Damme, R. V. Ham, B. Vanderborght, L. C. Visser, A. Bicchi, and A. Albu-Schffer, "Variable stiffness actuators: Review on design and components," *IEEE/ASME Transactions on Mechatronics*, vol. 21, no. 5, pp. 2418–2430, Oct 2016. doi: 10.1109/TMECH.2015.2501019

[7] G. Grioli, S. Wolf, M. Garabini, M. Catalano, E. Burdet, D. Caldwell, R. Carloni, W. Friedl, M. Grebenstein, M. Laffranchi, D. Lefeber, S. Stramigioli, N. Tsagarakis, M. Van Damme, B. Vanderborght, A. Albu-Schaeffer, and A. Bicchi, "Variable stiffness actuators: The user's point of view," *Int. J. Rob. Res.*, vol. 34, no. 6, pp. 727–743, May 2015.

[8] K.-H. Nam, B.-S. Kim, and J.-B. Song, "Compliant actuation of parallel-type variable stiffness actuator based on antagonistic actuation," *Journal of Mechanical Science and Technology*, vol. 24, no. 11, pp. 2315–2321, 2010. doi: 10.1007/s12206-010-0813-6. [Online]. Available: http://dx.doi.org/10.1007/s12206-010-0813-6

[9] G. Tonietti, R. Schiavi, and A. Bicchi, "Design and control of a variable stiffness actuator for safe and fast physical human/robot interaction," in *Robotics and Automation, 2005. ICRA 2005. Proceedings of the 2005 IEEE International Conference on*, April 2005. doi: 10.1109/ROBOT.2005.1570172 pp. 526–531.

[10] N. Tsagarakis, I. Sardellitti, and D. Caldwell, "A new variable stiffness actuator (CompAct-VSA): Design and modelling," in *Intelligent Robots and Systems (IROS), 2011 IEEE/RSJ International Conference on*, Sept 2011. doi: 10.1109/IROS.2011.6095006. ISSN 2153-0858 pp. 378–383.

[11] S. Groothuis, G. Rusticelli, A. Zucchelli, S. Stramigioli, and R. Carloni, "The Variable Stiffness Actuator vsaUT-II: Mechanical Design, Modeling, and Identification," *Mechatronics, IEEE/ASME Transactions on*, vol. 19, no. 2, pp. 589–597, April 2014. doi: 10.1109/TMECH.2013.2251894

[12] S. Wolf and G. Hirzinger, "A new variable stiffness design: Matching requirements of the next robot generation," in *Robotics and Automation, 2008. ICRA 2008. IEEE International Conference on*, May 2008. doi: 10.1109/ROBOT.2008.4543452. ISSN 1050-4729 pp. 1741–1746.

[13] J. Guo and G. Tian, "Conceptual design and analysis of four types of variable stiffness actuators based on spring pretension," *International Journal of Advanced Robotic Systems*, vol. 12, no. 5, p. 62, 2015. doi: 10.5772/60580. [Online]. Available: http://dx.doi.org/10.5772/60580

[14] ——, "Mechanical design and analysis of the novel 6-dof variable stiffness robot arm based on antagonistic driven joints," *Journal of Intelligent & Robotic Systems*, vol. 82, no. 2, pp. 207–235, 2016. doi: 10.1007/s10846-015-0279-y. [Online]. Available: http://dx.doi.org/10.1007/s10846-015-0279-y

[15] J. Hurst, J. Chestnutt, and A. Rizzi, "The actuator with mechanically adjustable series compliance," *Robotics, IEEE Transactions on*, vol. 26, no. 4, pp. 597–606, Aug 2010. doi: 10.1109/TRO.2010.2052398

[16] G. Spagnuolo, M. Malosio, T. Dinon, L. M. Tosatti, and G. Legnani, "Analysis and synthesis of linwwc-vsa, a variable stiffness actuator for linear motion," *Mechanism and Machine Theory*, vol. 110, pp. 85 – 99, 2017. doi: http://dx.doi.org/10.1016/j.mechmachtheory.2016.11.002. [Online]. Available: http://www.sciencedirect.com/science/article/pii/S0094114X16304700

[17] B. Vanderborght, N. G. Tsagarakis, R. Ham, I. Thorson, and D. G. Caldwell, "MACCEPA 2.0: Compliant Actuator Used for Energy Efficient Hopping Robot Chobino1D," *Auton. Robots*, vol. 31, no. 1, pp. 55–65, Jul. 2011.

[18] L. Fiorio, A. Parmiggiani, B. Berret, G. Sandini, and F. Nori, "PnrVSA: human-like actuator with non-linear springs in agonist-antagonist configuration," in *Humanoid Robots (Humanoids), 2012 12th IEEE-RAS International Conference on*, Nov 2012. doi: 10.1109/HUMANOIDS.2012.6651566. ISSN 2164-0572 pp. 502–507.

[19] D. Shin, X. Yeh, and O. Khatib, "Variable radius pulley design methodology for pneumatic artificial muscle-based antagonistic actuation systems," in *Intelligent Robots and Systems (IROS), 2011 IEEE/RSJ International Conference on*, Sept 2011. doi: 10.1109/IROS.2011.6095180. ISSN 2153-0858 pp. 1830–1835.

[20] A. Schepelmann, K. Geberth, and H. Geyer, "Compact nonlinear springs with user defined torque-deflection profiles for series elastic actuators," in *Robotics and Automation (ICRA), 2014 IEEE International Conference on*, May 2014. doi: 10.1109/ICRA.2014.6907350 pp. 3411–3416.

[21] M. Kilic, Y. Yazicioglu, and D. F. Kurtulus, "Synthesis of a torsional spring mechanism with mechanically adjustable stiffness using wrapping cams," *Mechanism and Machine Theory*, vol. 57, pp. 27 – 39, 2012. doi: http://doi.org/10.1016/j.mechmachtheory.2012.06.005. [Online]. Available: http://www.sciencedirect.com/science/article/pii/S0094114X12001334

[22] N. Hogan, "Adaptive control of mechanical impedance by coactivation of antagonist muscles," *Automatic Control, IEEE Transactions on*, vol. 29, no. 8, pp. 681–690, Aug 1984. doi: 10.1109/TAC.1984.1103644

Highlights

- The principle of operation of the RotWWC-VSA is presented.
- RotWWC-VSA is a multi-turn rotational variable stiffness actuator.
- The equations to analyze the mechanism are presented.
- Simulation results are given and commented.
- The concept design of a prototype embedding the RotWWC-VSA is described.